Optimized Deep Soil Mixing for Cutoff Walls in Tailings Dams: Correlating Laboratory Results with Field Performance

Nikolay Milev[1]*, Anton Sariev[2]

[1] Department of Geotechnics, University of Architecture, Civil Engineering and Geodesy (UACEG), 1 Hristo Smirnenski Blvd., Sofia 1164, Bulgaria

[2] GeoserviceEngineering AD, 9 Sava Katrafilov Str., Asenovgrad 4230, Bulgaria

*Corresponding author: **milev_fte@uacg.bg**

https://doi.org/10.5755/j01.sace.44131

JSACE 2/40

Optimized Deep Soil Mixing for Cutoff Walls in Tailings Dams: Correlating Laboratory Results with Field Performance

Received 2026/01/22

Accepted after revision 2026/04/12

Abstract

This study presents the concept, execution, and performance verification of a deep soil mixing (DSM) cutoff wall constructed at one of the largest copper tailings storage facilities (TSFs) in Europe, located in Bulgaria. The 500 m long wall, comprising 192 triple-panel DSM elements, was designed to mitigate seepage beneath a staged embankment raise. An integrated program combining laboratory optimization, field trials, and full-scale verification testing was implemented to ensure reliable performance under variable ground conditions. Laboratory mixing of representative tailings and gneissic soils with different binder contents identified an optimal formulation using blast furnace slag cement. Field trials confirmed that a two-cycle mixing procedure provided superior column uniformity. Verification testing of 66 boreholes across the completed barrier, including 198 unconfined compressive strength (UCS) and permeability tests, yielded hydraulic conductivities of 10-7–10-8 m/s and bulk densities of 1.8-2.0 g/cm^3. Statistical evaluation using the Bartlett-Kendall method indicated vertical homogeneity of strength, while lateral variability justified subdivision into three UCS zones. The resulting characteristic and design strengths confirm that the adopted DSM approach ensures both mechanical integrity and hydraulic efficiency for the investigated site conditions. Beyond the specific case study, the paper highlights an integrated laboratory–trial–verification workflow for the design and quality assurance of DSM cutoff walls in heterogeneous tailings deposits.

Keywords: blast furnace slag cement; cutoff wall; deep soil mixing (DSM); field verification; hydraulic conductivity; mix design optimization; statistical variability; tailings storage facility (TSF).

Introduction

Tailings storage facilities (TSFs) are critical components of the mining industry, ensuring the long-term management of large volumes of fine-grained waste materials. In recent decades, the increasing size of TSFs, combined with a series of catastrophic failures worldwide, has highlighted the need for improved design, monitoring, and risk mitigation strategies (Oboni & Oboni, 2020; Gupta & Kumar, 2023). One of the key challenges associated with TSFs is the control of seepage from the impounded tailings pond into the foundation and supporting dikes. Excessive infiltration can compromise the stability of the embankments, trigger internal erosion, and reduce the overall safety (Masengo et al., 2019).

In Bulgaria, one of the largest copper ore TSFs in Europe is undergoing staged expansion to accommodate future tailings deposition. The facility is a valley-type impoundment, founded on weathered gneiss, and supported by large rockfill embankments. To mitigate seepage beneath a

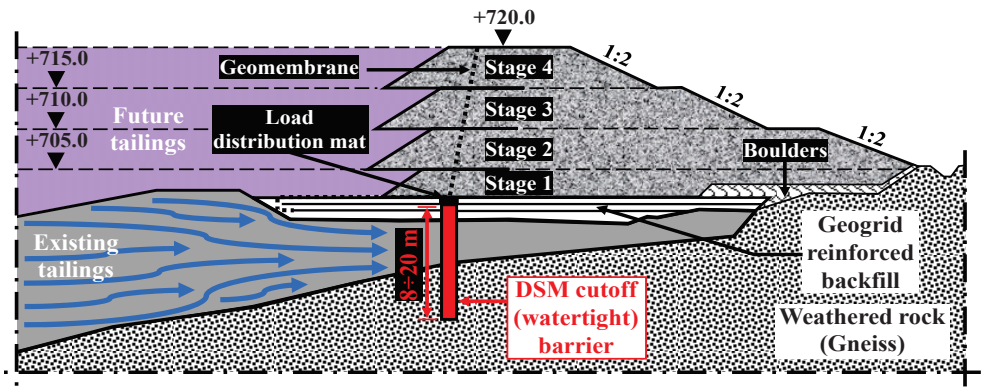
ktu 1922

Journal of Sustainable Architecture and Civil Engineering
Vol. 2 / No. 40 / 2026
pp. 131-145
DOI 10.5755/J01.SACE.44131

planned embankment raise, a continuous cutoff wall has been designed and executed using the deep soil mixing (DSM) method (Kitazume & Terashi, 2013; Nicholson, 2014). Unlike conventional soil improvement applications, this project involves constructing a vertical barrier through existing deposited tailings, which poses unique challenges due to their variable composition, compressibility, and hydraulic characteristics. A schematic cross-section of the overall concept is shown in Fig. 1.

The cutoff wall was constructed as a linear row of overlapping soil-cement columns, executed with a triple-axis DSM system. Each column has a diameter of 1000 mm and is installed at a center-to-center spacing of 880 mm, ensuring adequate overlap to form a continuous impermeable barrier (Bruce et al., 2013; European Committee for Standardization, 2006). The treatment depth ranges between 8 and 20 m, following the natural profile of the weathered gneiss and penetrating into it to ensure tight contact with the foundation. The total wall length is approximately 500 m, comprising 192 triple panels, forming a continuous barrier across the base of the future embankment. To integrate the barrier with the embankment system, a reinforced load distribution mat was constructed above the DSM columns. Around the wall, the foundation was further improved using geogrid-reinforced backfill, creating a solid base for the staged construction of the new embankment, which is planned to be raised in four stages, ultimately reaching an elevation of +720 m, thereby providing additional storage capacity for tailings deposition.

Fig. 1.
Schematic cross-section showing the DSM cutoff wall, load distribution mat, geogrid-reinforced backfill, and staged embankment raises up to elevation +720 m



The selection of DSM for this project is justified by several advantages: it enables in-situ treatment of heterogeneous tailings without excavation, minimizes disturbance to the existing deposit, and provides a continuous barrier with controllable hydraulic conductivity and mechanical strength (Al-Tabbaa, 2003; Topolnicki, 2016). However, the successful performance of DSM barriers depends critically on the mix design and execution parameters (Egorova et al., 2017; Hessouh et al., 2023). Recent studies have also shown that the relationship between laboratory-prepared and field-produced DSM material is not necessarily one-to-one, and that execution procedure may significantly influence both average strength and strength variability (Gonbad & Abdi, 2024). In this case, the non-traditional application of DSM in tailings necessitated a thorough program of preliminary verification. Representative samples of the in-situ tailings were retrieved using triple-tube core drilling and subjected to laboratory mixing trials. Different binder amounts and types were adopted in order to establish an optimal "recipe." Key parameters such as penetration and withdrawal rates, rotation speed, number of mixing cycles, and grout injection volume were evaluated in detail (Cement Deep Mixing Method Association, 1999; Fang et al., 2001).

Following field execution, verification was carried out by extracting cores from the DSM columns and performing unconfined compressive strength (UCS) tests. The field results were then interpreted in relation to the laboratory program, while recognizing the inherent differences between controlled laboratory specimens and full-scale DSM material produced under heterogeneous in-situ conditions (Esmaeili et al., 2014). This rigorous process ensured the creation of a low-permeability barrier with adequate strength to serve as an impermeable cutoff beneath the new embankment.

Although DSM is a mature ground-improvement method, published evidence remains limited for cutoff-wall applications in heterogeneous tailings deposits where representative laboratory strata, field mixing conditions, and full-scale barrier performance must be reconciled within one quality-assurance framework. The contribution of the present paper therefore does not lie in DSM as a method itself, but in the integrated verification workflow adopted for this tailings case: laboratory screening of representative strata and binders, field optimization of execution parameters, and full-scale hydraulic and mechanical verification combined with statistical interpretation of spatial variability. In this sense, the paper aims to contribute not only a well-documented case history, but also a structured methodology for the design and verification of DSM cutoff walls in non-traditional tailings environments.

The Deep Soil Mixing (DSM) Technique

The deep soil mixing (DSM) method originated in Japan and Scandinavia in the 1970s, initially developed as a ground improvement technique for soft clays and loose sandy soils (Van Impe, 1989; Kitazume & Terashi, 2013). Since then, DSM has gained worldwide recognition due to its versatility in reducing soil permeability, improving mechanical strength, and providing structural support for embankments, retaining walls, and foundation systems. The method has been widely adopted across Europe, particularly in Scandinavia, Germany, and the Netherlands, where it has been applied in a range of infrastructure and environmental protection projects. More recently, DSM technology has also become available in Bulgaria, opening opportunities for its application in challenging geotechnical projects, including large-scale tailings storage facilities. The technique involves in-situ treatment of the ground by injecting and blending a binder, typically a cement-based slurry, with the native soil using a set of rotating augers or mixing blades. Depending on the application, DSM can be executed as single shafts, overlapping columns, panels, or grids (Milev, 2023).

The effectiveness of the DSM process depends on a range of factors, including soil type, organic content, grain size distribution, and binder characteristics. These parameters directly influence the unconfined compressive strength (UCS) and permeability of the soil-cement mixture. A summary of the main factors governing the mechanical properties of treated soils is presented in Fig. 2.

For cutoff wall applications, DSM is most commonly applied in the form of secant or overlapping columns, producing a continuous low-permeability barrier (Pooranampillai et al., 2012). In the presented study, the method was implemented using a triple-shaft mixing system, which enables simultaneous installation of three 1000 mm diameter columns at a spacing of 880 mm. The construction process follows a well-established sequence, schematically illustrated in Fig. 3:

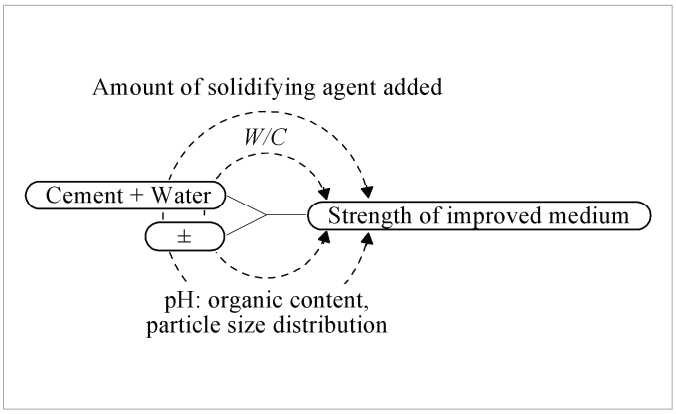


Fig. 2

Factors influencing the unconfined compressive strength (UCS) of soil-cement mixtures.

1. The equipment is positioned at the designated location of the planned column.
2. Drilling begins, with the mixing tool penetrating to the target depth.
3. During penetration, cement slurry is injected while blades or augers rotate, ensuring the slurry is blended with the in-situ soil (tailings).
4. Once the final depth is reached, additional mixing is carried out to guarantee uniform distribution of the slurry.
5. The mixing tool is then withdrawn, continuing to rotate and inject binder as needed to homogenize the soil-cement mixture throughout the column.
6. The tool is fully retracted, leaving behind the freshly formed soil-cement column, which subsequently hardens through cement hydration.

This sequence ensures homogeneity of the soil-binder mixture and reliable column continuity. An important advantage of DSM is its flexibility in forming different geometrical configurations of improved ground. Depending on project needs, DSM can be applied in block, lattice (grid), wall, or pile-type patterns. Wall-type configurations are particularly well-suited for seepage mitigation, as they allow the formation of continuous vertical barriers through heterogeneous soil layers. A schematic representation of single-shaft DSM execution, alongside its actual implementation at the studied tailings dam site in Bulgaria, is shown in **Fig. 4** (Milev, 2023).

Fig. 3

Execution sequence of the Deep Soil Mixing (DSM) method.

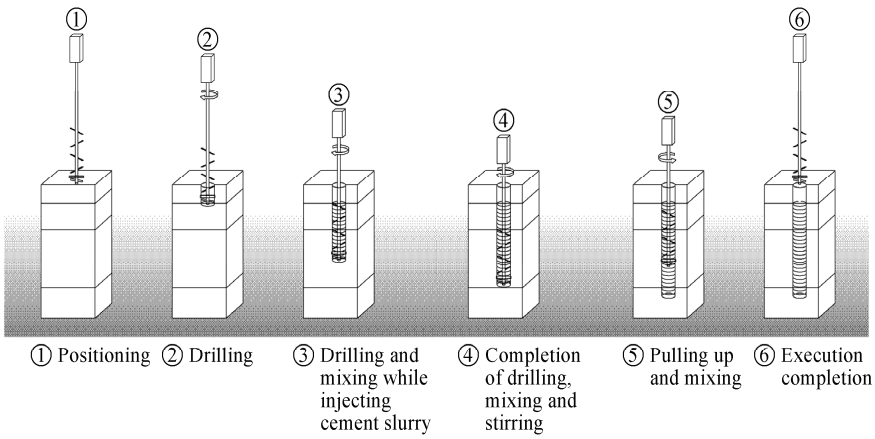
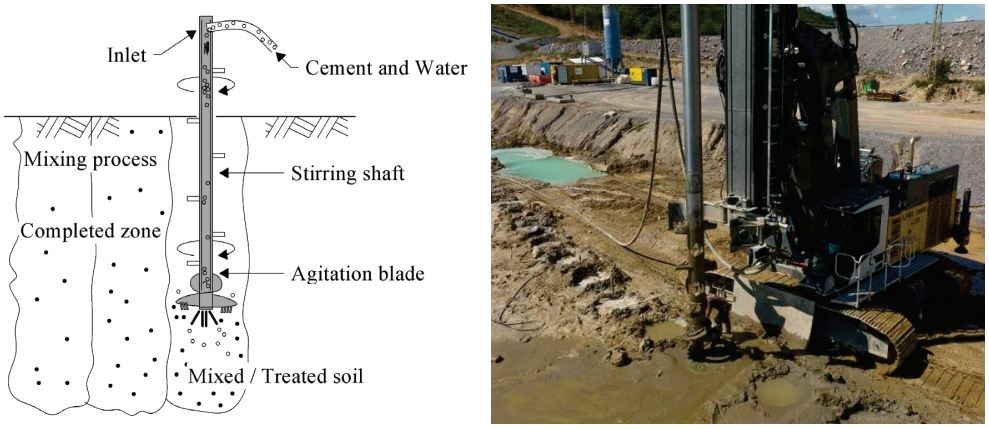


Fig. 4

Deep Soil Mixing (DSM): schematic representation of a single-shaft column (left) and actual execution at the tailings dam site in Bulgaria (right) – different zone.



While DSM has been extensively applied in natural soils, its use in tailings material remains limited. The variability of tailings composition, gradation, and mineralogy introduces uncertainties regarding the strength and permeability of DSM columns. In this study, the site-specific application of DSM in a large copper tailings facility required preliminary laboratory investigations to establish and optimize a reliable execution "recipe." Controlled mixing of retrieved tailings samples with different binder compositions and parameters was performed to guide the evaluation of expected field performance, later verified through core testing of executed columns. Such an approach is consistent with established DSM quality-control logic, in which laboratory mix testing, field trials, production control, and post-execution verification are treated as linked stages rather than isolated tasks (Kitazume & Terashi, 2013). The results underscore the importance of pre-execution testing when DSM is applied in non-traditional ground conditions such as tailings.

Laboratory Mix Design and Testing

Purpose and Procedure

The strength and permeability of soil-cement mixtures depend on many factors, including soil composition, water content, binder type and dosage, curing time, and mixing quality. For this reason, reliable mix design for deep soil mixing (DSM) projects cannot be established solely from preliminary soil investigations. Laboratory mix tests are essential for verifying binder efficiency and establishing an execution "recipe" representative of field application.

The purpose of the laboratory program was to establish an optimized mix-design envelope for the investigated tailings and foundation materials and to identify a binder formulation suitable for subsequent field trials and full-scale execution (Kanty et al., 2017). The laboratory stage was therefore conceived as a controlled screening and comparison phase rather than as an exact reproduction of field DSM execution. This distinction is important because laboratory-prepared specimens and field-produced DSM material are known to differ due to in-situ mixing conditions, soil heterogeneity, and construction-related variability (Kitazume & Terashi, 2013; Hessouh et al., 2023). In this study, soils were retrieved from three characteristic layers encountered during the site investigation. The first layer consists of tailings deposits varying in thickness between approximately 5 and 10 m. Beneath this, a second layer of weathered biotitic-muscovitic magmatized gneiss mixed with tailings extends over 3 to 8 m. Finally, the third layer is formed of fresh biotitic-muscovitic magmatized gneiss, which continued to the termination depths of the boreholes. Representative samples of each of these three soil types were treated separately in the laboratory. This separation was intended to isolate the relative influence of the principal strata encountered along the wall alignment, even though the field DSM process would later mix these materials along depth into a composite treated mass.

For stabilization, two types of cement were used: blast furnace slag cement (CEM III/A 42.5 N, denoted BFS) and ordinary Portland cement (CEM I 42.5 R, denoted OPC). These binders were selected to compare a conventional Portland cement reference with a slag-containing cement expected to provide favorable strength development under the fine-grained, water-rich tailings conditions encountered at the site. The water-to-cement ratio was kept constant at 1.0, reflecting common DSM slurry practice and allowing the effects of binder type and binder quantity to be compared without introducing an additional variable at the laboratory screening stage. Within this framework, mixtures were prepared with three levels of grout dosage (low, medium, and high) to capture the effect of binder quantity. In total, 88 cylindrical specimens with a diameter of 5.65 cm and a height of 11.3 cm (H/D ≈ 2.0; volume ≈ 283 cm^3) were produced and tested at curing periods of 14 and 28 days.

The proportions of soil, cement, and water for each specimen were derived from the mold volume and the measured natural water content of the soils. Based on these inputs, the required soil

mass was first established, after which the binder mass was calculated from the dry soil mass and the chosen binder factor. The quantity of slurry water was then determined using the fixed water-to-cement ratio of 1.0, identical to typical grout applied in the field. In some cases, additives were included as a percentage of the cement mass. This calculation framework, which is summarized in Table 1, ensures that the prepared specimens accurately represent the interaction between soil and grout expected during DSM execution.

Table 1

Mixture recipes and number of specimens prepared (soil, cement, and water proportions)

No.	Mix name based on: Cement content	Soil type	Binder type	Recipe Soil [g]	Cement [g]	Water [g]	Samples [pcs.]
1	I-1-BFC			3324	375	375	5
2	I-1-OPC			1994	225	225	0
3	II-1-BFC			3324	741	741	5
4	II-1-OPC			1994	445	445	3
5	III-1-BFC			3324	1108	1108	5
6	III-1-OPC			1994	665	665	0
7	I-2-BFC			5224	600	600	8
8	I-2-OPC			2612	300	300	4
9	II-2-BFC			5224	1186	1186	8
10	II-2-OPC			2612	593	593	4
11	III-2-BFC			5224	1772	1772	8
12	III-2-OPC			2612	886	886	3
13	I-3-BFC			5498	600	600	7
14	I-3-OPC			2749	300	300	4
15	II-3-BFC			5498	1186	1186	8
16	II-3-OPC			2749	593	593	4
17	III-3-BFC			5498	1772	1772	8
18	III-3-OPC			2749	886	886	4
			Σ:	64203	14233	14233	88

Soil types according to preliminary geotechincal report:

- **1 -** tailings
- **2 -** weathered biotitic to muscovitized magmatized gneisses, including tailings
- **3 -** biotitic to muscovitized magmatized gneisses

Legend:

- **I, II, III -** according to the cement content
- **1, 2, 3 -** according to the soil type
- **BFC -** blast furnace slag cement (CEM III/A 42.5 N)
- **OPC -** ordinary Portland cement (CEM I 42.5 R)

Table 2 presents the coding of the specimens, which reflects the soil type, cement type, curing time, and binder content per cubic meter. Each of the three soil layers (1, 2, and 3) was mixed with several binder quantities (I, II and III) to evaluate the influence of cement dosage on strength development. The target binder contents were 230 kg/m^3, 455 kg/m^3, and 680 kg/m^3, corresponding to low, medium, and high levels of treatment, respectively. Particular attention was paid to ensuring that the specified cement quantities represent the effective binder retained in the treated soil, accounting for the amount of material that is typically displaced during mixing. This approach enabled realistic replication of field conditions and ensured that lab results could be compared with in-situ DSM column performance. The selected dosage range was intended to capture a practical lower, intermediate, and upper bound of treatment intensity for subsequent field evaluation, rather than to imply that a single laboratory optimum could be transferred directly to production without field confirmation.

Specimen preparation followed adopted DSM laboratory specimen-preparation practice, with project-specific adaptations in mixing equipment and mold dimensions (Kitazume & Terashi, 2013). The retrieved soils were handled so as to preserve their natural water content prior to mixing. Mixing was carried out using a hand-held electric mixer with a spiral blade. The cement slurry was prepared separately and added gradually to the soil while mixing, with intermittent scraping of the mixer blades and bucket walls to limit segregation and improve uniformity. The total mixing time was approximately 10 min, divided into short intervals. The resulting mixtures were placed in molds in three layers, lightly compacted and de-aired by tapping. To compensate for volume loss

Table 2

Sample identification according to soil type, cement type, curing time, and binder content.

Soil type	Curing time (days)	Sample names according to cement type and binder amount					
		I		II		III	
		230 kg/m^3		455 kg/m^3		680 kg/m^3	
		BFC	OPC	BFC	OPC	BFC	OPC
1	14	I-1-BFC-14-1/2	-	II-1-BFC-14-1/2	-	III-1-BFC-14-1/2	-
		I-1-BFC-14-2/2		II-1-BFC-14-2/2		III-1-BFC-14-2/2	
	28	I-1-BFC-28-1/3	-	II-1-BFC-28-1/3	II-1-OPC-28-1/3	III-1-BFC-28-1/3	-
		I-1-BFC-28-2/3		II-1-BFC-28-2/3	II-1-OPC-28-2/3	III-1-BFC-28-2/3	
		I-1-BFC-28-3/3		II-1-BFC-28-3/3	II-1-OPC-28-3/3	III-1-BFC-28-3/3	
2	14	I-2-BFC-14-1/4	I-2-OPC-14-1/2	II-2-BFC-14-1/4	II-2-OPC-14-1/2	III-2-BFC-14-1/4	III-2-OPC-14-1/1
		I-2-BFC-14-2/4		II-2-BFC-14-2/4		III-2-BFC-14-2/4	
		I-2-BFC-14-3/4	I-2-OPC-14-2/2	II-2-BFC-14-3/4	II-2-OPC-14-2/2	III-2-BFC-14-3/4	
		I-2-BFC-14-4/4		II-2-BFC-14-4/4		III-2-BFC-14-4/4	
	28	I-2-BFC-28-1/4	I-2-OPC-28-1/2	II-2-BFC-28-1/4	II-2-OPC-28-1/2	III-2-BFC-28-1/4	III-2-OPC-28-1/2
		I-2-BFC-28-2/4		II-2-BFC-28-2/4		III-2-BFC-28-2/4	
		I-2-BFC-28-3/4	I-2-OPC-28-2/2	II-2-BFC-28-3/4	II-2-OPC-28-2/2	III-2-BFC-28-3/4	III-2-OPC-28-2/2
		I-2-BFC-28-4/4		II-2-BFC-28-4/4		III-2-BFC-28-4/4	
3	14	I-3-BFC-14-1/4	I-3-OPC-14-1/2	II-3-BFC-14-1/4	II-3-OPC-14-1/2	III-3-BFC-14-1/4	III-3-OPC-14-1/2
		I-3-BFC-14-2/4		II-3-BFC-14-2/4		III-3-BFC-14-2/4	
		I-3-BFC-14-3/4	I-3-OPC-14-2/2	II-3-BFC-14-3/4	II-3-OPC-14-2/2	III-3-BFC-14-3/4	III-3-OPC-14-2/2
		I-3-BFC-14-4/4		II-3-BFC-14-4/4		III-3-BFC-14-4/4	
	28	I-3-BFC-28-1/4	I-3-OPC-28-1/2	II-3-BFC-28-1/4	II-3-OPC-28-1/2	III-3-BFC-28-1/4	III-3-OPC-28-1/2
		I-3-BFC-28-2/4		II-3-BFC-28-2/4		III-3-BFC-28-2/4	
		I-3-BFC-28-3/4	I-3-OPC-28-2/2	II-3-BFC-28-3/4	II-3-OPC-28-2/2	III-3-BFC-28-3/4	III-3-OPC-28-2/2
				II-3-BFC-28-4/4		III-3-BFC-28-4/4	

during early shrinkage, the molds were slightly overfilled and then sealed for curing. The quantities of the constituent materials were documented for each mix. A visual illustration of the mixing setup, process, and specimen preparation is presented in Fig. 5.



Fig. 5

Laboratory mixing setup: materials and tools (left), mixing process with hand-held machine in bucket (middle), and prepared specimens in molds (right).

Unconfined compressive strength (UCS) tests were performed on all stabilized specimens to examine the effects of soil type, binder type, binder content, and curing time. The laboratory results were later interpreted together with UCS tests on cores retrieved from trial and production DSM columns in the field. In this way, the laboratory program served as a decision-support stage for binder selection and dosage screening, while final acceptance of the adopted execution parameters relied on field verification of continuity, homogeneity, and mechanical performance.

Results and Interpretation

The results of the unconfined compressive strength (UCS) tests on the stabilized specimens are presented in Fig. 6, which illustrates the variation of UCS with curing time for the three representative soil types. Fig. 7 shows the corresponding development of the secant deformation modulus.

Fig. 6

Unconfined compressive strength (UCS) versus curing time for stabilized specimens: (left) soil type 1 – tailings, (middle) soil type 2 – weathered gneiss with tailings, (right) soil type 3 – fresh gneiss.

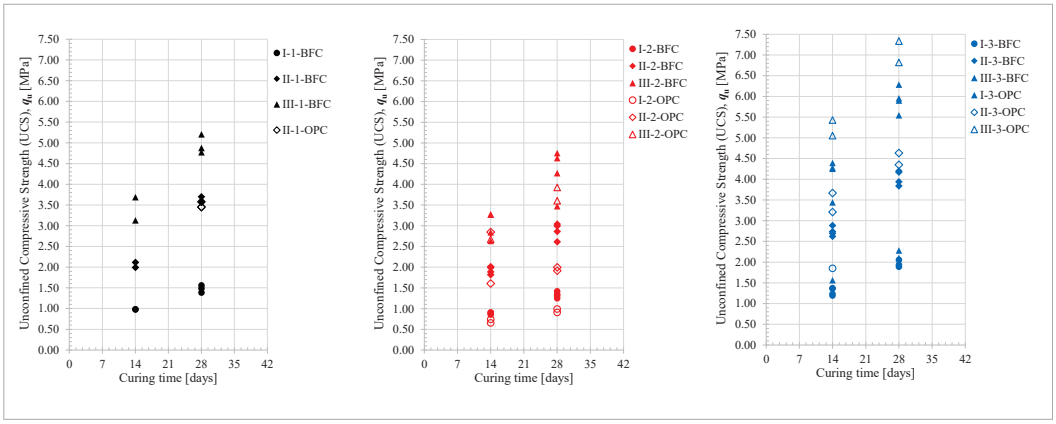
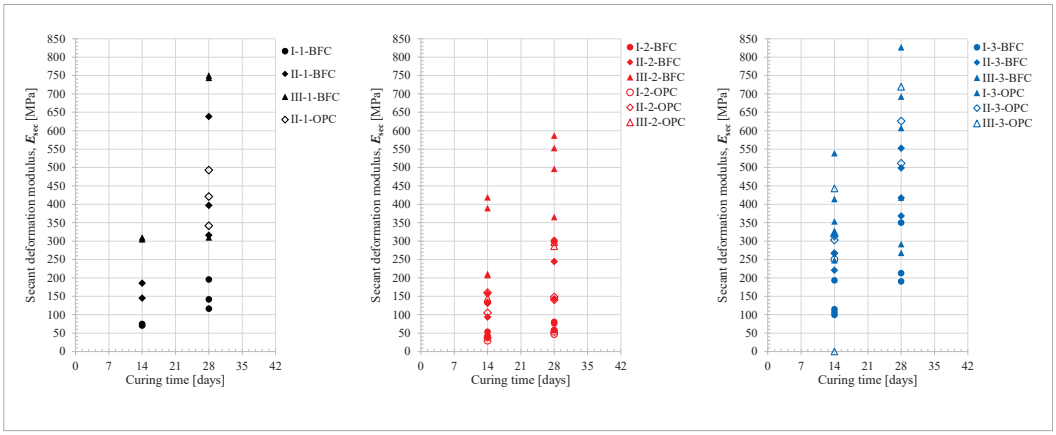


Fig. 7

Secant deformation modulus versus curing time for stabilized specimens: (left) soil type 1 – tailings, (middle) soil type 2 – weathered gneiss with tailings, (right) soil type 3 – fresh gneiss.



The overall trends in both figures are consistent, confirming the progressive gain in stiffness and strength with increasing binder content and curing time.

As expected, the UCS of the stabilized specimens increased with higher binder dosage for all three soil types. Mixtures prepared with the highest binder content (680 kg/m^3) consistently exhibited the greatest strength, followed by those with medium (455 kg/m^3) and low (230 kg/m^3) binder quantities. This proportional increase confirms that binder quantity was a primary control on laboratory strength development within the investigated dosage range, although its effect remained dependent on the characteristics of the treated soil.

Curing time also had a significant influence on strength development. Between 14 and 28 days, the UCS values increased markedly for all mixtures, reflecting the continued hydration of cementitious compounds and the progressive formation of cement-soil bonds. The increase was most pronounced in the tailings (Soil "1") and weathered gneiss with tailings (Soil "2"), which initially had higher water contents and finer particle sizes, conditions that were more favorable for slurry distribution and subsequent strength gain under the adopted mixing procedure.

The comparison between the two cement types revealed a distinct trend: for Soil "1" and Soil "2", the specimens stabilized with blast furnace slag cement (CEM III/A 42.5 N, BFS) achieved noticeably higher UCS values than those treated with ordinary Portland cement (CEM I 42.5 R, OPC). At the engineering level, this behavior is consistent with the generally favorable performance of slag-containing binders in fine-grained and water-rich materials. In contrast, for the fresh gneiss (Soil "3"), the OPC-based mixtures performed slightly better, likely due to the lower reactivity and coarser texture of the mineral matrix, which favor faster early hydration typical of Portland cement. It should be noted, however, that the present study did not include mineralogical

or microstructural analyses – therefore, these explanations are offered as engineering interpretations of the observed strength trends rather than as direct mechanistic proof.

Considering the overall performance across all soil types and the field application requirements, BFS was selected as the preferred binder for the cutoff wall. Its superior performance in the more critical upper layers (Soils "1" and "2") outweighed the marginal difference observed in the deeper gneissic layer. From a practical standpoint, this made BFS the more suitable choice for subsequent field trials. In addition, slag-containing binders are often regarded as advantageous in large-scale DSM works because of their lower heat evolution and potential environmental relevance in practice. However, the present study did not include a formal durability assessment or environmental evaluation, and these aspects are therefore interpreted qualitatively only.

Based on the laboratory results, the upper boundary binder content of approximately 680 kg/m^3 was adopted as the preferred laboratory reference level for subsequent field evaluation, providing a conservative basis for assessing strength development and execution robustness. At 28 days, the average UCS across all specimens and soil types was approximately 5.06 MPa, which is considered satisfactory for the intended function of the DSM barrier as an impermeable cutoff wall. At the same time, the laboratory results were interpreted as part of a staged decision process rather than as a stand-alone acceptance criterion, because final parameter selection depended on field verification of column continuity, homogeneity, and hydraulic performance under actual execution conditions.

Field Verification and Performance Evaluation

Trial Columns and Optimization of Field Parameters

Before commencing large-scale execution of the DSM cutoff wall, a trial field program was carried out to verify the laboratory results and optimize the execution parameters under actual site conditions. Unlike the laboratory stage, where the three representative soil layers were treated separately, in the field the DSM process unavoidably mixes the materials encountered along the penetration depth into a continuous, homogenized soil-cement mass. Consequently, the field performance cannot be directly compared to the laboratory specimens on a one-to-one basis. However, the laboratory results provided a valuable reference for estimating the expected strength range and guiding the selection of binder quantities and mixing conditions. In this sense, the field trial program served as an intermediate decision stage between laboratory screening and full-scale execution, allowing the selected laboratory mix-design envelope to be examined under actual production conditions.

The field trials were performed in a designated test area, separate from the main cutoff wall alignment. Six test DSM column types, labeled A-F, were executed with varying binder contents, water-cement ratios, and mixing procedures, as summarized in Table 3. The objective was to identify the optimal combination of binder dosage and execution parameters ensuring uniform strength and integrity along the full column depth. Accordingly, the trial evaluation considered not only the measured UCS values, but also the visual integrity of the recovered cores, the continuity of the treated mass, and the quality of the overlap zones, which are critical for a wall-type seepage barrier.

The binder contents ranged from 456 kg/m^3 (Type A) to 1 045 kg/m^3 (Type F). For all trials, the injection rate was maintained at 400 l/min, while the penetration and withdrawal rates were kept constant at 0.20 m/min and 1.80 m/min, respectively. The main variables were the number of penetration/withdrawal cycles and the water-cement (W/C) ratio (which directly influenced grout density). Columns A-E were executed using a single penetration/withdrawal cycle (I), whereas Type F involved two full penetration/withdrawal cycles (II) – the first conducted slowly to ensure binder penetration and the second at a faster withdrawal rate of 1.8 m/min to promote homogenization and improve column continuity.

Table 3

Mixing parameters and characteristics of trial DSM column types depending on mixing technique and binder amount.

Mixing parameters	Unit	Test DSM column types depending on mixing technique and binder amount													
		A		B		C		D		E		F			
		456 kg/m³		745 kg/m³		672 kg/m³		539 kg/m³		488 kg/m³		1 045 kg/m³			
		Penetration (P) and Withdrawal (W) cycles (I or II)													
		I-P	I-W	I-P	I-W	I-P	I-W	I-P	I-W	I-P	I-W	I-P	I-W	II-P	II-W
Water–cement ratio (W/C)	-	2.0	1.0	1.0		1.7	0.8	1.5	1.0	1.7	1.0	0.8			
Grout density	g/cm³	1.31	1.52	1.52		1.35	1.61	1.39	1.52	1.35	1.52	1.61			
Injection rate	l/min	400													
Penetration / withdrawal rate	m/min	0.20	1.80	0.20	1.80	0.20	1.80	0.20	1.80	0.20	1.80	0.20	1.80		

The photographs presented in Fig. 8 illustrate the visual differences between extracted cores from Type C and Type F. The cores were retrieved using a triple-tube HQ3 sampling system. While Type C samples exhibited discontinuities, cracks, and partial segregation, Type F cores appeared dense, continuous, and uniform along their entire length, indicating superior mixing quality and binder distribution.

Fig. 8

Field core samples from trial DSM columns: Type C (left) showing discontinuities and partial segregation, and Type F (right) showing uniform, well-cemented structure.



Verification testing was performed on cores extracted from the overlapping zones of the triple-axis columns, corresponding to the most conservative part of the improved ground, where mixing between adjacent columns is most critical – Fig. 9 (right). Three depth intervals were tested in each column type, approximately 4.0-4.5 m, 10.0-10.5 m, and 15.0-15.5 m, to assess the vertical uniformity of mechanical performance. The measured unconfined compressive strengths (UCS) at 28 days are summarized and plotted in Fig. 9 (left). The purpose of this verification step was therefore not only to compare strength levels between trial variants, but also to assess the degree to which different execution procedures produced a continuous and uniform treated zone at the most critical overlap locations.

The UCS results confirmed the general trend observed in the laboratory: higher binder contents produced greater strength. However, due to natural heterogeneity and the mixing of all soil types in situ, the results exhibited more variability. Columns B and C showed slightly higher average UCS values (up to 6.7 MPa) than Type F. Nonetheless, field observations revealed that the corresponding cores contained multiple discontinuities, soft zones, and cracked segments, suggesting incomplete homogenization. Conversely, Type F columns displayed consistently uniform structure and fewer defects, even though their UCS values (ranging between 2.9 MPa and 4.2 MPa) were marginally lower. This comparison indicates that, although Types B and C achieved higher local peak strengths, their structural continuity and homogenization were less reliable. By contrast, Type F provided a more uniform treated mass and more consistent overlap quality, which are of primary importance for cutoff wall performance. For such applications, local maximum UCS values alone are not a sufficient basis for selecting the final execution procedure if they are accompanied by discontinuities that may impair hydraulic continuity.

Based on this assessment, Type F was selected as the final configuration for the cutoff wall. The adopted parameters included a binder content of 1 045 kg/m³, a water-cement ratio of 0.8, grout density of 1.61 g/cm³, and two full penetration-withdrawal cycles. Although the resulting UCS was slightly below the highest values observed in the laboratory and in some single-cycle trial

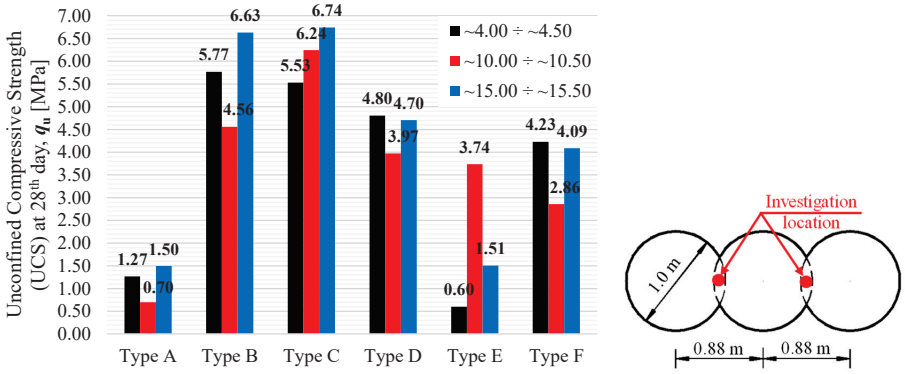


Fig. 9

Unconfined compressive strength (UCS) of test DSM columns at 28 days for different depths (left) and schematic location of core sampling in column overlap zone (right).

columns, the visual integrity of the recovered cores, the reduced occurrence of defects, and the improved uniformity of the overlap zones indicated that this configuration provided the best overall balance between adequate strength, homogeneity, continuity, and constructability under field conditions. The final selection was therefore based on barrier performance criteria in the engineering sense, rather than on peak UCS values alone.

Verification Testing of Executed DSM Columns

Verification testing was performed in the working zone along the entire cutoff-wall alignment, approximately 500 m in length. A total of 66 boreholes were drilled at regular intervals, each yielding six core specimens extracted from the middle of the overlapping zones of the triple-shaft DSM columns, which represent the most critical locations. From each borehole, three specimens were tested for hydraulic conductivity and three for unconfined compressive strength (depths of approximately 4.0-4.5 m, 10.0-10.5 m, and 15.0-15.5 m), while bulk density was also determined on representative fragments of the cores. This sampling strategy was intentionally conservative, because the overlap zones govern continuity of the barrier and are therefore the most critical portions of a wall-type DSM system. At the same time, it should be recognized that such a strategy focuses verification on the most critical locations and does not capture every possible local fluctuation within the total treated mass.

Hydraulic conductivity was measured in the laboratory on saturated specimens under a controlled hydraulic gradient of 2.5 bar, following a constant-head approach suitable for low-permeability materials. The resulting coefficients were of the order of 10^{-7}–10^{-8} m/s, confirming that the executed DSM barrier satisfies the target impermeability. The bulk density of the treated material ranged between 1.8 and 2.0 g/cm^3, consistent with a dense and well-hydrated soil-cement matrix. Taken together, these results indicate that the completed wall achieved the intended hydraulic function under the tested conditions, while also providing indirect support for adequate mixing and curing of the treated material.

In order to assess the uniformity of strength along the height of the DSM columns, the Bartlett-Kendall statistical method was applied to the dataset of 198 UCS results obtained at depths of 5, 10, and 15 m (Bartlett, 1937; Kendall, 1947). The analysis indicated no statistically significant difference in variance between depths ($p \approx 0.20$), implying that UCS values are vertically consistent. This result is consistent with the use of a uniform execution technique and with the mixing-induced homogenization expected for the investigated wall geometry. However, the absence of statistically significant depth-related differences in the sampled dataset should be interpreted as evidence of no detectable vertical trend within the tested intervals, rather than as proof of complete uniformity throughout the entire wall. On this basis, subdivision of the wall height into strength-dependent layers was not considered necessary for design purposes.

In contrast, the lateral variation of UCS along the cutoff wall was found to be more pronounced. The results plotted in Fig. 10 clearly illustrate this trend, showing the 28-day UCS values along the 500 m wall. As seen in the figure, UCS gradually decreases with distance, as captured by the regression line (R^2 = 0.23). Although this regression trend is moderate, the spatial pattern was considered sufficiently consistent for engineering interpretation. The purpose of the analysis was not detailed geostatistical modeling, but the definition of practical strength zones reflecting the observed lateral variability of the executed wall. On this basis, the wall was subdivided into three representative strength zones (Zone 1, Zone 2, and Zone 3), corresponding to high, intermediate, and low UCS levels, respectively.

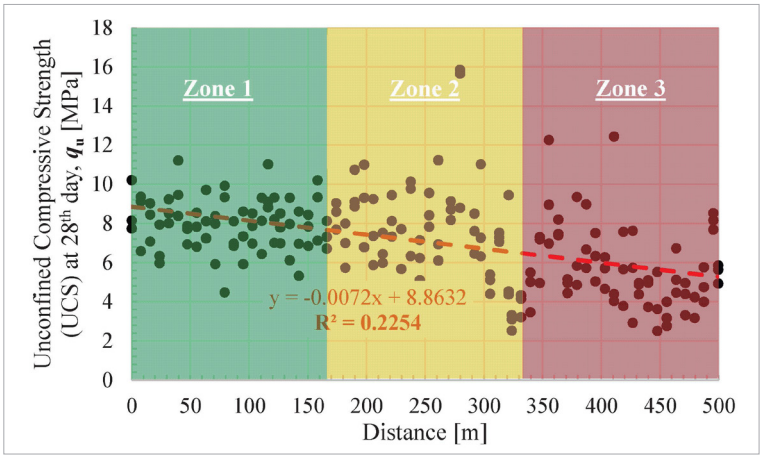


Fig. 10
Spatial distribution of 28-day unconfined compressive strength (UCS) along the cutoff-wall alignment, showing linear trendline and zoning boundaries (Zone 1 – high UCS, Zone 2 – intermediate, Zone 3 – low).

Because of this lateral variability, a single characteristic UCS value for the entire wall would not be representative. Therefore, the characteristic UCS for each zone was determined according to Eurocode 7, such that at least 95% of the measured values exceed the characteristic value (Bond & Harris, 2006; European Committee for Standardization, 2007; Frank et al., 2004). The resulting characteristic strengths are 7.6 MPa (Zone 1), 5.8 MPa (Zone 2), and 4.5 MPa (Zone 3). Applying the partial material factor γ^M = 1.5 and the coefficient α^{cc} = 0.85 gives design compressive strengths of 4.3 MPa, 3.3 MPa, and 2.6 MPa for Zones 1, 2, and 3, respectively. This zoned treatment was adopted to obtain design values that better reflect the observed field behavior, rather than to suggest abrupt material boundaries in a geological sense.

For numerical and structural analysis, the design tensile strength can be conservatively estimated as one-tenth of the design compressive strength. Accordingly, the adopted design tensile strengths are approximately 0.43 MPa for Zone 1, 0.33 MPa for Zone 2, and 0.26 MPa for Zone 3. These zoned parameters capture the main lateral variation observed in the executed DSM wall, while the lack of a detectable depth-dependent trend in the sampled dataset supports the assumption of uniform design values along the column height. More broadly, the verification results indicate that full-scale DSM performance in heterogeneous tailings should be interpreted probabilistically and spatially, rather than through a single deterministic strength value for the entire barrier.

Discussion

The results of this study demonstrate that the deep soil mixing (DSM) technique can be effectively applied for seepage control in tailings storage facilities when laboratory optimization and field execution are properly integrated. More specifically, the present case study highlights the value of a staged laboratory–trial–verification workflow for wall-type DSM barriers constructed in heterogeneous tailings and weathered gneiss conditions. The laboratory investigation established a consistent relationship between binder type, dosage, and strength development, confirming that blast furnace slag cement (BFS) provides superior strength development in fine-grained tailings compared to ordinary Portland cement. From an engineering standpoint, this performance advantage is consistent with the favorable behavior of slag-containing binders in fine-grained and water-rich materials. However, since no mineralogical or microstructural analyses were performed,

this interpretation should be regarded as an engineering explanation of the observed trends rather than as direct mechanistic proof.

Field observations emphasized that the energy and thoroughness of mixing are critical factors in achieving column uniformity and continuity. The comparison of trial columns revealed that two full penetration-withdrawal cycles yielded a more homogeneous soil-cement mass, while single-cycle procedures, despite locally higher strengths, produced discontinuities and weaker bonding. This finding indicates that, for cutoff wall applications, DSM quality cannot be judged on the basis of nominal binder quantity or peak local UCS alone. Continuity of the treated mass and the integrity of the overlap zones are equally important, because local defects may compromise the hydraulic function of the barrier even when isolated strength values are high. In this sense, the selection of Type F reflects a barrier-performance criterion rather than simple strength maximization.

Verification testing confirmed the robustness of the adopted methodology. The measured hydraulic conductivities align with benchmark values reported for well-executed DSM barriers, validating the cutoff wall's hydraulic performance. The statistical evaluation using the Bartlett-Kendall approach indicated no significant vertical strength variation, confirming consistent execution quality along the column height. In contrast, a gradual lateral decrease in UCS along the wall length reflected natural variability in tailings density and binder distribution. Subdividing the wall into three representative strength zones provided a rational means to incorporate this variability into design calculations, ensuring realistic and conservative performance assessment. At the same time, the verification results should not be interpreted as eliminating uncertainty. The field dataset remains influenced by natural heterogeneity of the tailings and weathered foundation, by the known differences between laboratory-prepared specimens and field-produced DSM material, and by the limitations of core-based sampling. In addition, the adopted coring strategy was focused on the overlap zones, which are the most critical parts of the barrier, but this also means that the dataset does not represent every possible local fluctuation within the total treated mass. Such spatial variability is consistent with the broader understanding that cement-mixed columns may exhibit heterogeneity across different observational scales (Wong et al., 2024).

Overall, the integrated laboratory-field approach confirmed that DSM cutoff walls can achieve both mechanical and hydraulic reliability in challenging tailings environments when the material formulation, execution parameters, and statistical verification are coherently managed. However, the findings should be interpreted within the limits of a single-site case study. The proposed workflow, representative laboratory screening, field optimization, and full-scale verification, may be transferable to other TSFs, but the resulting binder selection, strength development, and design values will remain site-specific and may vary with tailings composition, mineralogy, groundwater chemistry, and execution system. Likewise, although the use of in-situ treatment and slag-containing cement may be regarded as favorable from a practical sustainability perspective, the present study did not include a formal life-cycle or environmental assessment – therefore, any sustainability implication should be interpreted qualitatively only, whereas stronger sustainability claims in deep mixing are typically supported by explicit life-cycle assessment (Kravchenko et al., 2024).

Conclusions

This study demonstrates that deep soil mixing (DSM) can be a reliable technique for constructing cutoff walls in large tailings dams. The integration of systematic laboratory mix design, optimized field execution, and extensive verification testing ensured consistent performance for the investigated site conditions of the barrier.

The findings emphasize three essential aspects of successful DSM application: the superior strength development and practical suitability of blast furnace slag cement in tailings environments; the critical importance of double-cycle mixing for achieving column uniformity; and the value of statistical verification in identifying and managing spatial variability.

By introducing a zoned framework grounded in measured field variability, the project established a rational basis for defining characteristic and design parameters consistent with Eurocode 7 principles. This data-driven approach bridges the gap between laboratory predictions and field performance, ensuring both mechanical integrity and hydraulic efficiency. In this respect, the contribution of the study lies not in DSM as a new method, but in the structured laboratory–field verification workflow adopted for a wall-type barrier constructed in heterogeneous tailings conditions.

Ultimately, this case study contributes to advancing the understanding and practical implementation of DSM in complex tailings materials. It shows that, through rigorous laboratory-field integration and statistical control, DSM cutoff walls can provide a reliable and well-verified solution for seepage mitigation under such conditions. The conclusions should, however, be interpreted within the limits of a single-site case study. The proposed workflow may be transferable to other tailings storage facilities, but the resulting material behavior and design values remain site-specific and depend on local geology, tailings characteristics, groundwater conditions, and execution system. Uncertainty and spatial variability remain inherent in full-scale DSM applications, and the resulting design values should therefore be interpreted within the limits of the investigated site and execution system. Although the adopted solution may have practical sustainability relevance due to in-situ treatment and the use of slag-containing cement, the present study did not include a formal environmental assessment; this aspect should therefore be interpreted qualitatively only.

References

Al-Tabbaa, A. (2003). Soil mixing in the UK 1991-2001: state of practice report. Proceedings of the Institution of Civil Engineers-Ground Improvement, 7(3), 117-126. https://doi.org/10.1680/grim.2003.7.3.117

Bartlett, M. S. (1937). Properties of sufficiency and statistical tests. Proceedings of the royal society of london. series a-mathematical and physical sciences, 160(901), 268-282. https://doi.org/10.1098/rspa.1937.0109

Bond, A., & Harris, A. (2006). Decoding Eurocode 7. CRC Press. https://doi.org/10.1201/9781482265873

Bruce, M. E. C., Berg, R. R., Filz, G. M., Terashi, M., Yang, D. S., Collin, J. G., & Geotechnica, S. (2013). Federal Highway Administration design manual: Deep mixing for embankment and foundation support (No. FHWA-HRT-13-046). United States. Federal Highway Administration. Offices of Research & Development.

Cement Deep Mixing Method Association. (1999). Cement Deep Mixing Method (CDM). Design and Construction Manual (in Japanese).

Egorova, A. A., Rybak, J., Stefaniuk, D., & Zajączkowski, P. (2017, October). Basic aspects of deep soil mixing technology control. In IOP conference series: materials science and engineering (Vol. 245, No. 2, p. 022019). IOP Publishing. https://doi.org/10.1088/1757-899X/245/2/022019

Esmaeili, M., Gharouni-Nik, M., & Khajehei, H. (2014). Evaluation of deep soil mixing efficiency in stabilizing loose sandy soils using laboratory tests. Geotechnical Testing Journal, 37(5), 817-827. https://doi.org/10.1520/GTJ20130099

European Committee for Standardization. (2006). EN 14679:2006 - Execution of special geotechnical works - Deep mixing. Brussels: CEN.

European Committee for Standardization. (2007). EN 1997-2:2007 - Eurocode 7: Geotechnical design - Part 2: Ground investigation and testing. Brussels: CEN.

Fang, Y. S., Chung, Y. T., Yu, F. J., & Chen, T. J. (2001). Properties of soil-cement stabilized with deep mixing method. Proceedings of the Institution of Civil Engineers-Ground Improvement, 5(2), 69-74. https://doi.org/10.1680/grim.2001.5.2.69

Frank, R., Bauduin, C., Driscoll, R. M., Kavvadas, M., Ovesen, N. K., Orr, T., ... & Gulvanessian, H. (2004). Designers' Guide to Eurocode 7: Geotechnical Design: Designers' Guide to EN 1997-1. Eurocode 7: Geotechnical Design-General Rules (Vol. 17). Thomas Telford.

Gonbad, M. S. S., & Abdi, M. R. (2024). Influence of mixing time and execution procedure on strength characteristics of improved sand using deep soil mixing (DSM) method. Construction and Building Materials, 448, 138115. https://doi.org/10.1016/j.conbuildmat.2024.138115

Gupta, S., & Kumar, S. (2023). A state-of-the-art review of the deep soil mixing technique for ground improvement. Innovative Infrastructure Solutions, 8(4), 129. https://doi.org/10.1007/s41062-023-01098-6

Hessouh, J. J., Eslami, J., Beaucour, A. L., Noumowe, A., Mathieu, F., & Gotteland, P. (2023). Physical and mechanical characterization of deep soil mixing (DSM) materials: Laboratory vs construction site. Construc-

tion and Building Materials, 368, 130436. https://doi.org/10.1016/j.conbuildmat.2023.130436

Kanty, P., Rybak, J., & Stefaniuk, D. (2017, October). Some remarks on practical aspects of laboratory testing of deep soil mixing composites achieved in organic soils. In IOP Conference Series: Materials Science and Engineering (Vol. 245, No. 2, p. 022018). IOP Publishing. https://doi.org/10.1088/1757-899X/245/2/022018

Kendall, M. G. (1947). The Advanced Theory Or Statistics. C. Griffin.

Kitazume, M., & Terashi, M. (2013). The deep mixing method (Vol. 21). London: CRC press. https://doi.org/10.1201/b13873

Kravchenko, E., Lu, W., Sauerwein, M., & Wong, A. H. (2024). Life cycle assessment of waste materials in deep cement mixing for land reclamation in Hong Kong. Environmental Impact Assessment Review, 105, 107398. https://doi.org/10.1016/j.eiar.2023.107398

Masengo, E., Julien, M. R., Lavoie, P., Lépine, T., Nousiainen, J., Saukkoriipi, J., ... & Karvo, J. (2019). Enhancement of contractive tailings using deep soil mixing technique at Kittilä mine. In Sustainable and Safe Dams Around the World/Un monde de barrages durables et sécuritaires (pp. 3396-3409). CRC Press. https://doi.org/10.1201/9780429319778-306

Milev, N. (2023). Soil liquefaction countermeasures. Sofia: Kolbis International Transfer Corp.

Nicholson, P. G. (2014). Soil improvement and ground modification methods. Butterworth-Heinemann. https://doi.org/10.1016/B978-0-12-408076-8.00012-1

Oboni, F., & Oboni, C. (2020). Tailings dam management for the twenty-first century. Berlin/Heidelberg, Germany: Springer International Publishing. https://doi.org/10.1007/978-3-030-19447-5

Pooranampillai, S., Parmantier, D., Dawson, K., & Shin, S. (2012). A case history on the design, construction, and field quality control of cement Deep Soil Mixing. In 37th Annual conference on deep foundations (pp. 135-145).

Topolnicki, M. (2016). General overview and advances in Deep Soil Mixing. In XXIV geotechnical conference of torino design, construction and controls of soil improvement systems (pp. 25-26).

Van Impe, W. F. (1989). Soil improvement techniques and their evolution.

Wong, D. Y. C., Sadasivan, V., Isaksson, J., Karlsson, A., & Dijkstra, J. (2024). Trans-scale spatial variability of lime-cement mixed columns. Construction and Building Materials, 417, 135394. https://doi.org/10.1016/j.conbuildmat.2024.135394

About the authors

NIKOLAY MILEV

Associate Professor

Department of Geotechnics (Faculty of Transportation Engineering), University of Architecture, Civil Engineering and Geodesy (UACEG)

Main research area

Soil dynamics, liquefaction assessment, and soil improvement

Address

1 Hristo Smirnenski Blvd., Sofia 1164, Bulgaria
E-mail: milev_fte@uacg.bg

ANTON SARIEV

Technical Director

GeoserviceEngineering AD

Main research area

Soil improvement and complex drilling technologies

Address

9 Sava Katrafilov Str., Asenovgrad 4230, Bulgaria
E-mail: a.sariev@gse.bg

This article is an Open Access article distributed under the terms and conditions of the Creative Commons Attribution 4.0 (CC BY 4.0) License (http://creativecommons.org/licenses/by/4.0/).